# Development of Regulatory Audit Codes for Performance Analysis of Cr-coated ATF Fuel

Joosuk Lee, Hyedong Jeong, Sarah Kang, Seulbeen Kim, Jang Keun Park, Byunggil Huh, Yongseok Choi
*Korea Institute of Nuclear Safety*
*62 Gwahak-ro, Yusong-gu, Daejeon, 305-338, Republic of Korea*
*Tel: +82-42-868-0784, Fax: +82-42-868-0045*
*Email: jslee2@kins.re.kr*

## 1. Introduction

KEPCO Nuclear Fuel (KNF), Korea Atomic Energy Research Institute (KAERI), and Korea Hydro & Nuclear Power (KHNP) are actively engaged in the development of various Accident Tolerant Fuels (ATF) for use in Pressurized Water Reactors (PWR) [1]. Among the ATF concepts Cr-coated zircaloy cladding shows promise for near-term application. Although it shares similar mechanical and neutronic properties with zirconium alloys, notable distinctions, particularly in corrosion characteristics, arise due to the Cr coating layer [1,2]. From a pellet perspective, KNF has developed a $UO_2$ pellet with large grain structure, incorporating $La_2O_3$-$Al_2O_3$-$SiO_2$ (LAS). Concurrently, KNF and KHNP are planning to load this ATF fuel into the PWR core as Lead-Test-Rod (LTR) in 2024 and Lead-Test-Assembly (LTA) in 2025 [3,4].

To ensure core safety from a regulatory standpoint, the development of regulatory audit methodologies, including computer codes, becomes crucial. In this context, the authors previously conducted a scoping safety analysis of Cr-Coated ATF cladding, employing additional models in FRAPCON-KS and FAMILY computer codes [5]. FRAPCON-KS is a modified version of FRAPCON4.0P1 in KINS tailored for the application of HANA and Cr-coated HANA cladding. FAMILY represents an integrated code between MARS-KS and FRAPTRAN, and some improvements applied.

Recently, KINS has acquired preliminary material properties of Cr-coated cladding from the ATF consortium in Korea [6]. Using this and literature survey, detailed models for the application of FRAPCON-KS and FAMILY codes have been under developing. Additionally based on these codes, the steady-state and transient fuel performance during a Loss of Coolant Accident (LOCA) are preliminarily evaluated. This study introduces the developed models and properties briefly, and outcomes of fuel performance analysis.

## 2. Models and Properties

The Cr-coated cladding developed by KNF is based on the HANA-6 zirconium alloy substrate [3]. Consequently, the majority of material properties and correlations differ from those of Zircaloy-4 or ZIRLO modeled in FRAPCON/FAMILY. Table 1 presents the developed models and properties for application in FRAPCON-KS and FAMILY.

Table 1 List of implemented models and properties for Cr-coated ATF cladding in FRAPCON-KS and FAMILY

| Models and Properties |
|---|
| Cladding thermal conductivity |
| Cladding thermal expansion |
| Cladding elastic modulus |
| Cladding creep |
| Cladding specific heat |
| Cladding emissivity ($Cr_2O_3$ layer) |
| Cladding axial growth |
| Cladding Meyer hardness |
| Cladding yield stress |
| Cladding waterside corrosion |
| Cladding hydrogen pickup |
| Cladding high temperature oxidation |
| Cladding high temperature creep |
| $Cr_2O_3$ thermal conductivity |
| $Cr_2O_3$ specific heat |

Basically, material properties of ATF cladding, such as thermal conductivity, thermal expansion, elastic modulus, specific heat, emissivity, etc., exhibit variances compared to ZIRLO/Zircaloy-4, although the differences are not significant. However, performance aspects such as cladding thermal creep, waterside corrosion, and high-temperature oxidation significantly differ from those observed in conventional ZIRLO/Zrcaloy-4 cladding [1,6]. Following descriptions provide an overview of some developed models [7].

- ***Waterside corrosion:*** Following initial parabolic oxidation kinetics, the oxide thickness was reduced to approximately one-tenth of the ZIRLO cladding model (EPRI-NP-5100) [5].
- ***Thermal creep:*** Thermal creep was minimized to several tens of the ZIRLO cladding model to induce a minimal amount of thermal creep [6].
- ***High-temperature oxidation:*** As described in the authors' previous works [5], the following oxidation kinetic model in steam environment is implemented to take into account the protective effects of $Cr_2O_3$ [8]. This may remain valid until complete consumption of the Cr-coating layer.

$$k_p = 2.69\text{x}10^{-3}\exp(-120{,}000/RT)\ [\text{m/s}^{0.5}]$$

*where, R = gas constant, 8.314 [J/mol-K]*
*T = temperature [K]*

- ***High temperature creep and burst:*** The high-temperature creep deformation model of HANA-6 cladding is adopted due to limited data on ATF cladding. Concerning cladding burst strain, NUREG-0630 burst strain criteria are also applied due to limited data [9].

## 3. Modeling for Performance Analysis

The 16x16 PLUS7 fuel, consisting ZIRLO/$UO_2$ and Cr-coated HANA-6/LAS-added $UO_2$, in the APR1400 reactor, were modeled for steady-state and LOCA safety analyses. Utilizing the FRAPCON-KS and FAMILY codes, which are incorporating the models and properties outlined in Table 1, the evaluation of steady-state and transient fuel performance during the LOCA period was conducted. Steady-state fuel performances were assessed up to 60 MWd/kgU, while the LOCA safety analysis was performed at a fuel burnup of 30 MWd/kgU, as it represents the most limiting condition from a peak cladding temperature (PCT) perspective [10].

For the LOCA analysis, the APR1400 reactor core was segmented into one hot channel and one average channel, with a single fuel rod allocated in the hot channel. This fuel rod was divided into 40 evenly spaced axial nodes. The local peak fuel power was set to 9.8 kW/ft for steady-state and 14.1 kW/ft before the LOCA accident. Constraints on cladding deformation due to adjacent fuel rod contact were implemented. When the cladding hoop strain at a specific axial node reached 78.6% (based on the outer diameter of the cladding), plastic deformation at the node ceased, and the deformation propagated in the axial direction.

The high-temperature cladding creep model for ZIRLO in FAMILY was slightly modified. This may result in different performance analysis comparing to the previous authors' work [5]. The strain-based NUREG-0630 fast ramp criterion was employed for cladding burst evaluation [9]. The assumed grain size of the LAS-added $UO_2$ pellet was set to 20 μm, and a modified Massih model was used for fission gas release assessment [11].

An uncertainty analysis was also conducted, accounting for fuel and thermal-hydraulic uncertainties, with detailed parameter descriptions available in reference 12. A non-parametric statistical method was employed to quantify the uncertainty PCT and equivalent cladding reacted (ECR). The Carthcart-Pawel oxidation model for zirconium alloys was utilized for measuring the ECR [13]. Employing a simple random sampling method, 124 inputs were generated, and calculations were performed.

## 4. Fuel Performance Assessment

### *4.1 Steady-state fuel performance*

A comparison of fuel performance between ZIRLO and Cr-coated ATF cladding fuel is presented in Fig. 1 and 2. In Fig. 1(a), the evolution of $ZrO_2$ and $Cr_2O_3$ oxide thickness is depicted, reaching up to 56.1 μm and 6.2 μm, respectively, at 60 MWd/kgU. Fig. 1(b) illustrates the minimum gap thickness between the pellet and cladding. From the start of burning to 1 MWd/kgU, the minimum gap thickness increases due to pellet densification. As fuel burning progresses further, continuous inward cladding creep occurs, finally resulting in cladding contact. Cladding contact initiates at 17 MWd/kgU for ZIRLO and 26 MWd/kgU for ATF cladding. The delayed contact in ATF cladding is attributed to its lower thermal creep characteristics. Fig. 1(c) depicts changes in stored energy. Maximum stored energies are observed in fresh fuel condition for both claddings. As fuel burning commences, stored energies decrease in both claddings, with ZIRLO cladding fuel displaying lower energy than ATF fuel. Minimum energies are observed at 11 MWd/kgU for ZIRLO and 16 MWd/kgU for ATF fuel. Beyond these burnups, energies increase. After a burnup of 15 MWd/kgU, ZIRLO fuel exhibits slightly higher energy than ATF fuel, possibly due to differences in oxide layer thickness.

In Fig. 2(a), changes in fission gas release (FGR) are shown. 1 % FGR in ZIRLO with $UO_2$ fuel is observed at 23 MWd/kgU, increasing to 6.3% at 60 MWd/kgU. Meanwhile, 1 % FGR is observed at 39 MWd/kgU in Cr-coated ATF fuel with LAS added $UO_2$, reaching
.

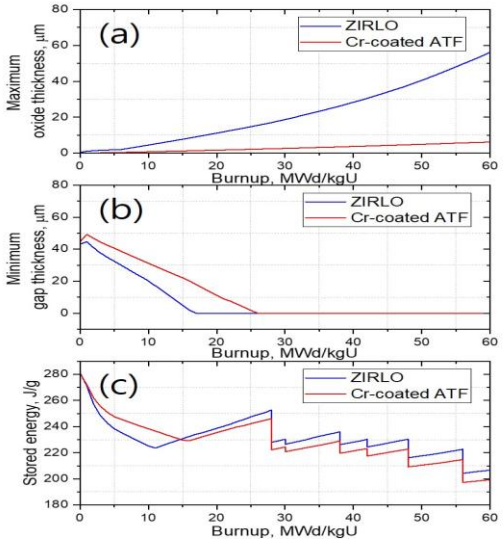


Fig.1. Comparison of (a) oxide thickness, (b) cladding permanent hoop strain and (c) stored energy between ZIRLO and simulated Cr-coated ATF cladding.

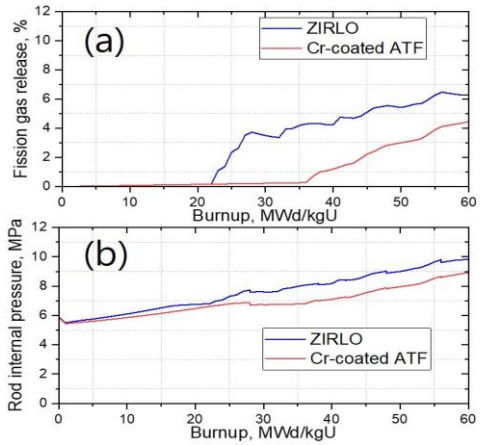


Fig.2. Comparison of (a) oxide thickness, (b) cladding permanent hoop strain and (c) stored energy between ZIRLO and simulated Cr-coated ATF cladding.

4.4 % at 60 MWd/kgU. The lower FGR in ATF fuel is attributed to the larger grain size of the LAS-added $UO_2$ pellet. Fig. 2(b) displays the evolution of rod internal pressure (RIP). At 1 MWd/kgU, RIP is 5.5 MPa in ZIRLO cladding with $UO_2$ fuel, increasing continuously to 9.8 MPa at 60 MWd/kgU. In Cr-coated ATF cladding with LAS-added $UO_2$ fuel, 5.4 MPa RIP is observed at 1 MWd/kgU, reaching 8.9 MPa RIP at 60 MWd/kgU. The lower RIP in ATF fuel is attributed to the lower FGR and lower fuel temperature. The assessed fuel performances in ATF fuel appear reasonably consistent with the implemented.

*4.2 Transient fuel performance*

Fig. 3 illustrates the evolution curves of PCT during a LOCA. For ZIRLO cladding fuel, as shown in Fig. 3(a), the base case blowdown and reflood PCT values are 1177.3 K and 1087.5 K, respectively. Among the 124 cases assessed, the third-highest blowdown and reflood PCT values are 1295.8 K and 1201.3 K, respectively. For Cr-coated ATF fuel, depicted in Fig. 3(b), the base case blowdown and reflood PCT values are 1152.3 K and 1085.1 K, respectively. The third-highest blowdown and reflood PCT values are 1258.7 K and 1173.0 K. These mean that the ATF fuel can result in a reduction of 25.0 K and 2.4 K in the base case blowdown and reflood PCT, respectively. Moreover, the third-highest PCT values in the blowdown and reflood phases are also reduced by 37.1 K and 28.3 K, respectively.

Fig. 4 presents the 124 ECR evolution curves during LOCA. For ZIRLO cladding fuel, as depicted in Fig. 4(a), the base case ECR is 1.3 %. Among the 124 cases assessed, the highest ECR value is 5.7 %. On the other hand, in the case of Cr-coated ATF fuel shown in Fig. 4(b), the base case ECR is 0.3 %, and the highest ECR is 1.7 %. These results indicate that the use of ATF cladding can lead to a reduction of 1.0 percentage point (o/p) and 4.0 o/p of ECR for the base case and 124 random samplings, respectively.

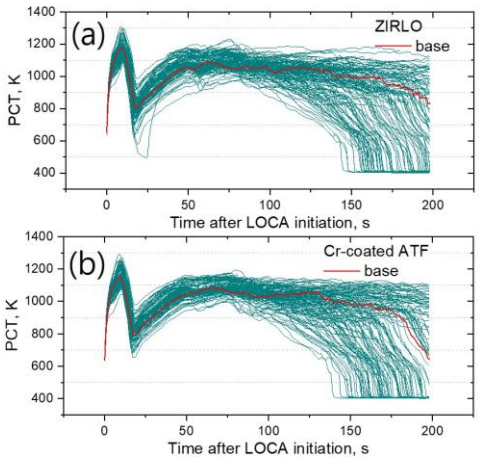


Fig. 3. Evolution of 124 PCT curves during LOCA, (a) ZIRLO and (b) Cr-coated ATF cladding

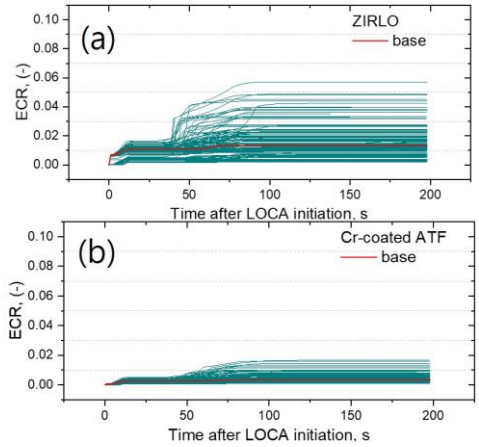


Fig. 4. Evolution of 124 ECR curves during LOCA, (a) ZIRLO and (b) Cr-coated ATF cladding

The changes in PCT and ECR between conventional and ATF fuel are influenced by various factors. However, main factors appear to include stored energy in the fuel, temperature rise in the oxide layer, Metal-Water reaction energy in the cladding, plastic deformation of the cladding, and the resultant relocation of fuel, among others. A more detailed analysis and the development of robust models may be required for further study.

## 5. Summary

Regulatory audit codes of FRAPCON-KS and FAMILY for Cr-Coated ATF were developed and performance analysis during steady-state and LOCA was conducted preliminarily. The following findings were obtained:

- Various material properties and models specific to Cr-coated ATF fuel were successfully developed

and implemented in the regulatory audit codes of FRAPCON-KS and FAMILY.

- In steady-state fuel performance, the stored energy in Cr-coated ATF fuel is generally lower than that in conventional ZIRLO/$UO_2$ fuel, except below ~15 MWd/kgU burnup ranges. Additionally, the oxide thickness formed outside the cladding and the rod internal pressure are also lower than in ZIRLO/$UO_2$ fuel.
- During LOCA, Cr-coated ATF fuel exhibits lower PCT and ECR values compared to ZIRLO/$UO_2$ fuel. This reduction can be attributed to factors such as decreased initial oxide thickness, stored energy, Metal-Water reaction energy, and plastic deformation. However, a more detailed analysis is required to identified this.

Based on the current preliminary analysis, Cr-coated ATF fuel developed in Korea for near-term application seems to enhance fuel safety during both steady-state and LOCA conditions. Nevertheless, further detailed and robust model development, grounded in experimental evidence, is essential for the refinement of regulatory audit codes.

## REFERENCES

[1] 이종선, 원전운영자 관점에서의 사고저항성연료 개발 방향 제언, 사고저항성핵연료: 단기 및 장기전략 워크샵, 2022.5 제주

[2] Brachet J.-C. et al., High temperature steam oxidation of chromium-coated zirconium-based alloys: Kinetics and process, Corrosion Science, art. no. 108537, 2020

[3] KNF, ATF 시범연료봉 장전노심 안전성 평가, KNF-TR-DM-23003 Rev0, 2023.4, Proprietary

[4] KNF, ATF 시범집합체 장전노심 안전성 평가, KNF-TR-DM-24001 Rev0, 2024.1, Proprietary

[5] Joosuk Lee et.al, Development of Regulatory Audit Methodologies for Cr-coated ATF Cladding: A Scoping Analysis on LOCA Safety, KNS Spring meeting, Jeju, 2023

[6] KNF, Material Properties of ATF Cladding, email communication, 2023.7

[7] Joosuk Lee et.al., Development of Basic Regulatory Audit Technology for Safety Analysis of ATF LTR, KINS/RR-2434, 2023.12

[8] Brachet J.-C. et al., Evaluation of Equivalent Cladding Reacted paramenters of Cr-coated claddings oxidized in steam at 1200 C in relation with oxygen diffusion/partitioning and post-quench ductility, Journal of Nuclear Materials, art. no. 152106, 2020

[9] Power, D.A., Meyer, R.O., Cladding Swelling and Rupture Models for LOCA Analysis. U.S. NRC, NUREG-0630, 1980

[10] Joosuk Lee, Young Seok Bang, Effects of fuel relocation on fuel performance and evaluation of safety margin to 10CFR50.46c ECCS acceptance criteria in APR1400 plant, Nuclear Engineering and Design 397 (2022) 111945

[11] K.J. Geelhood et. al., "FRAPCON-4.0: A Computer Code for the Calculation of Steady-State, Thermal-Mechanical Behavior of Oxide Fuel Rods for High Burnup", PNNL-19418, Vol.1. Rev.2, September 2015

[12] Joosuk Lee, Young-Seok Bang, Evaluation of core-wide fuel pin burst during LOCA in APR1400, Nuclear Engineering and Design 371 (2021) 110955

[13] Cathcart, J., et al., Zirconium metal–water oxidation kinetics, IV: reaction rate studies, ORNL/NUREG-17, 1977